Short-time dynamics of monomers and dimers in quasi-two-dimensional colloidal mixtures

Erick Sarmiento-Gómez,[1,*] José Ramón Villanueva-Valencia,[2] Salvador Herrera-Velarde,[3] José Arturo Ruiz-Santoyo,[2] Jesús Santana-Solano,[4] José Luis Arauz-Lara,[1] and Ramón Castañeda-Priego[2,†]

[1]*Instituto de Física "Manuel Sandoval Vallarta," Universidad Autónoma de San Luis Potosí, Alvaro Obregón 64, 78000 San Luis Potosí, SLP, México*

[2]*División de Ciencias e Ingenierías, Campus León, Universidad de Guanajuato, Loma del Bosque 103, 37150 León, México*

[3]*Subdirección de Postgrado e Investigación, Instituto Tecnológico Superior de Xalapa, Sección 5A Reserva Territorial s/n, 91096 Xalapa, Veracruz, México*

[4]*Cinvestav Unidad Monterrey, Parque de Investigación e Innovación Tecnológica, Apodaca, 66629 Nuevo León, México*

(Received 21 December 2015; revised manuscript received 4 May 2016; published 11 July 2016)

We report on the short-time dynamics in colloidal mixtures made up of monomers and dimers highly confined between two glass plates. At low concentrations, the experimental measurements of colloidal motion agree well with the solution of the Navier-Stokes equation at low Reynolds numbers; the latter takes into account the increase in the drag force on a colloidal particle due to wall-particle hydrodynamic forces. More importantly, we find that the ratio of the short-time diffusion coefficient of the monomer and that of the center of mass of the dimmer is almost independent of both the dimer molar fraction, x_d, and the total packing fraction, ϕ, up to $\phi \approx 0.5$. At higher concentrations, this ratio displays a small but systematic increase. A similar physical scenario is observed for the ratio between the parallel and the perpendicular components of the short-time diffusion coefficients of the dimer. This dynamical behavior is corroborated by means of molecular dynamics computer simulations that include explicitly the particle-particle hydrodynamic forces induced by the solvent. Our results suggest that the effects of colloid-colloid hydrodynamic interactions on the short-time diffusion coefficients are almost identical and factorable in both species.

DOI: 10.1103/PhysRevE.94.012608

I. INTRODUCTION

Many phenomena observed in colloidal dispersions resemble those in atomic systems. However, the colloidal dynamics exhibits special features due to solvent-mediated forces typically known as hydrodynamic interactions (HIs) [1]. Contrary to direct particle-particle interactions, HIs can be tuned, but never completely screened or switched off. In a simple physical picture, HIs can be understood as follows. The motion of a given colloidal particle induces a flow field in the solvent which is felt by the surrounding colloids. Thus, the motion of one colloidal particle causes a solvent-mediated force on the neighboring colloidal particles.

In contrast to its static counterpart, colloidal dynamics is far from being completely understood. The reason is partially related to the fact that the colloidal dynamics extends over a wide range of temporal and length scales due to the enormous difference in size and mass between the colloids and the solvent molecules, giving rise to complex and long-ranged HIs [1,2]. The latter lead to nontrivial coupling among colloids that extends over many mean interparticle distances [1,2]. The understanding of HIs is thus of relevance not only in physics, but also in several branches of science, such as biology, since phenomena like hydrodynamic synchronization in either biological systems (sperm, cilia, flagella) [3,4] or active fluids [5] and the dynamics of microswimmers [6,7] can only be explained in terms of hydrodynamic forces.

During the last few decades, the study of hydrodynamic coupling between two or three spherical colloids [8,9] or a spherical colloid near a wall [10–12] has been made possible, thanks to the use of videomicroscopy techniques [13] and the optical control of colloids through focused beams of light [8]. Besides, the contribution of HIs to the colloidal dynamics at finite concentration has been mainly studied in model monodisperse suspensions composed of spherical colloids in the bulk [2] and confined between two plates or at the air-water interface [14–17]. Nonetheless, a few years ago, the dynamical behavior of anisotropic colloids started to be experimentally studied at low particle concentrations [18–20]. However, little is known about the effects of HIs in multicomponent systems made up of spherical [21] and nonspherical colloids; this kind of mixture offers richer and interesting dynamical behavior. Recent contributions point mainly toward the study of hydrodynamic coupling between the translational and the rotational degrees of freedom of a family of nonspherical colloids [22] and the short-time diffusivity of dicolloidal particles [23]. Nevertheless, nowadays, we still lack of a full understanding of the effects of the HIs in multicomponent anisotropic colloidal systems in an extended window of particle concentrations.

In this contribution, we report on the short-time dynamics in quasi-two-dimensional colloidal mixtures composed of monomers and dimers. Our results make it evident that HIs affect the short-time dynamics in such a way that the diffusion coefficient can be decomposed into two contributions: one including only confinement effects, in the form of a diffusion coefficient at infinite dilution different from the bulk value, and the other a monotonically decreasing part that depends only on the volume fraction. Moreover, we give experimental and simulation evidence that the functional form of the latter contribution is almost identical, factorable, and independent of the particle composition for both species up to

*esarmiento@ifisica.uaslp.mx
†ramoncp@fisica.ugto.mx

concentrations around $\phi \sim 0.5$. At higher concentrations, this scenario changes slightly.

The idea that the effects of HIs on the self-diffusion of colloidal particles can be decoupled and factorable started almost 30 years ago with the pioneering contribution of Medina-Noyola [24], who theoretically studied the long-time self-diffusion coefficient in concentrated colloidal dispersions and assumed that it can be decomposed into two parts: one related to the short-time dynamics and the other depending only on the direct interactions between colloids. The main assumptions behind this original proposal have been applied in the self-consistent generalized Langevin approximation [24], which has been successfully used to account for the dynamics of several colloidal systems. Recently, Thorneywork *et al.* [17] experimentally demonstrated that the long-time dynamics does not depend crucially on HIs and is dominated by direct (hard-core) interactions, but simultaneously illustrated that the short-time dynamics depends on the area fraction, pointing to a significant contribution by HIs at short times. We here provide evidence that the short-time self-diffusion coefficient, D^s, can also be decomposed into well-defined contributions. In particular, we show further below that the D^s of each species can be expressed as

$$D_i^s = D_i^0 D_i^w(d) D_i^{cc}(\phi), \tag{1}$$

where i stands for either monomer (m) or dimer (d), D^0 is the free particle diffusion in the bulk, D^w is a contribution of the HIs that depends only on the separation of the glass plates, d, and $D^{cc}(\phi)$ is the contribution due to particle-particle hydrodynamic forces. More importantly, we observe that D^{cc} is almost identical for both species and is thus factorable.

II. EXPERIMENTAL SETUP

Colloidal dimers are prepared following the aggregation and fractionation procedure described in Ref. [25]. Polystyrene (spherical) particles of diameter $\sigma = 2$ μm (Duke Scientific) with negatively charged sulfate end groups on the surface, in a water solution, are dialyzed against ultrapure water. Particle aggregation is promoted by the addition of NaCl at a concentration of 500 mM during 6 min. This process is quenched by dialysis of the colloidal suspension in clean water. To produce sinterization of particles in contact, a vial with the suspension is immersed in glycerol at a temperature close to the melting temperature of polystyrene (104°C) for 15 min. After cooling down at room temperature (24° ± 0.1°C), the different colloidal clusters are separated by centrifugation in a sugar density gradient tube; sugar is eliminated by centrifugation and redispersion in an aqueous solution of SDS at 1 cmc to avoid further clusterization. The resulting dimers are then mixed with monomers and a small amount of larger particles, diameter 2.98 μm, which serve as spacers. This protocol has proved that the resulting interaction potential among colloids is of the hard-sphere type [25]. The colloidal dispersion is confined between two clean glass plates (a slide and a coverslip). The system is sealed with epoxy resin and the mobile particles are allowed to equilibrate in the confined geometry. A schematic of the quasi-two-dimensional system is displayed in Fig. 1(a).

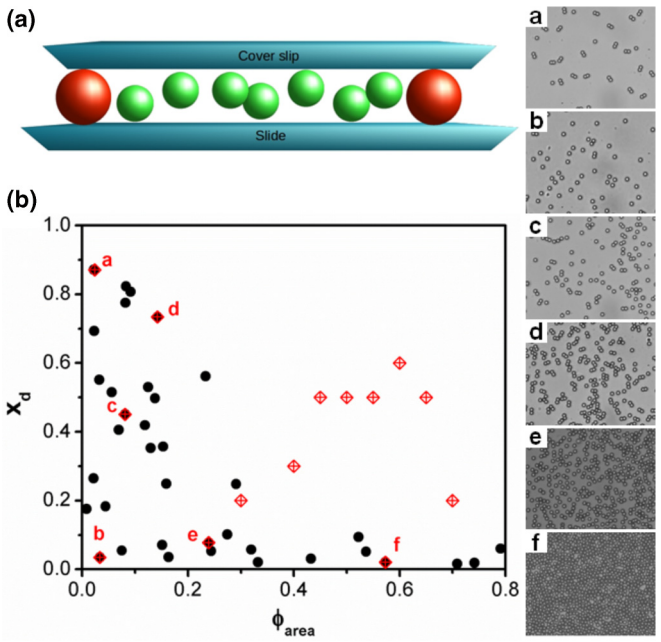

FIG. 1. (a) Cartoon of the colloidal mixture of monomers and dimers confined between two glass plates separated by spacers. (b) Experimental (circles) and simulated (diamonds) points in the parameter space, x_d vs ϕ, considered in this work. Inset: Snapshots (a–f) of experimental equilibrium configurations.

In order to track the colloidal particles, the sample is observed from the top view, i.e., perpendicular to the glass walls, using an optical microscope with a 40× objective and numerical aperture 0.6. The time evolution of the system is recorded using standard video equipment [26]. Because of the high confinement of the mixture, the motion of the particles perpendicular to the walls is greatly restricted. Individual images extracted from the recorded video are analyzed to obtain both x and y coordinates of the center of the particles, and from these data the trajectories are fully recovered. Dimers are identified by tracking the average distance between adjacent particles as a function of time. We have found the average distance between the centers of particles forming dimers to be $0.9\sigma \pm 0.04\sigma$, as a consequence of the sinterization procedure. From the trajectories, both translational and rotational components of the mean-square displacements (MSDs) are obtained. In the case of the dimers, the translational MSD can also be decomposed into the directions parallel and perpendicular to the long axis of symmetry.

The previous protocol is carried out for several dimer molar fractions x_d and total packing fractions ϕ in order to explore a wide number of points in the parameters space, as displayed in Fig. 1(b). For comparison of experimental measurements with computer simulations, we have selected six representative points in the parameters space [diamonds labeled a–f in Fig. 1(b)]. We also explored a few additional points through molecular dynamics (MD) simulations to extend our results even for those state points that were not experimentally accessible. In particular, we have chosen equimolar ($x_d \sim 0.5$) state points to cover the interval $0.5 < \phi < 0.7$.

III. DIFFUSION AT LOW CONCENTRATIONS: WALL-PARTICLE HYDRODYNAMIC FORCES

It is well known that HIs and the Brownian motion of colloidal particles are dramatically affected by the presence of walls [12,27]. In particular, several experiments have been carried out to understand single-particle diffusion near a flat wall [28–30]. Furthermore, Rice and coworkers derived a robust approximation to determine the decrease in the diffusion coefficient parallel to the walls at infinite dilution, which was corroborated in experiments on an isolated colloidal sphere confined between flat plates [28]. Basically, they consider that in the bulk, i.e., far away from the walls, the short-time dynamics of a colloid is characterized by the Stokes-Einstein diffusion coefficient $D^0 = k_B T/3\pi\eta\sigma$, where k_B is the Boltzmann constant, T the absolute temperature, and η the solvent viscosity. However, near the wall, a colloid experiences changes in the drag force due to the wall-particle hydrodynamic forces, which lead to a reduction in the short-time self-diffusion coefficient by a factor [28]

$$\frac{1}{\lambda(z)} = \left[1 - \frac{9}{16}\left(\frac{a}{z}\right) + \frac{1}{8}\left(\frac{a}{z}\right)^3 - \frac{45}{256}\left(\frac{a}{z}\right)^4 - \frac{1}{16}\left(\frac{a}{z}\right)^5\right], \tag{2}$$

where z is the perpendicular distance between the center of the sphere and the wall and a is the radius of the monomers [see Fig. 2(a)]. Nevertheless, under the experimental conditions, a colloid feels the effects of two walls. We then assume that each spherical colloid moves exactly at the middle of the two parallel flat walls [see Fig. 2(b)] and that the drag forces can be superimposed linearly. Thus, it is possible to obtain an approximate value for the short-time diffusion coefficient of a single sphere under confinement. Using the parameters of the experiments, this approximation predicts a reduction of 45% in the short-time diffusion coefficient of a single sphere at the bulk. This prediction is close to the experimental value measured for monomers under very diluted conditions [low finite concentration; Fig. 1(b)], whose reduction is about 35% the value of D_m^0; $D_m^s/\sigma^2 = (0.01821 \pm 7 \times 10^{-5})\ \mathrm{s}^{-1}$.

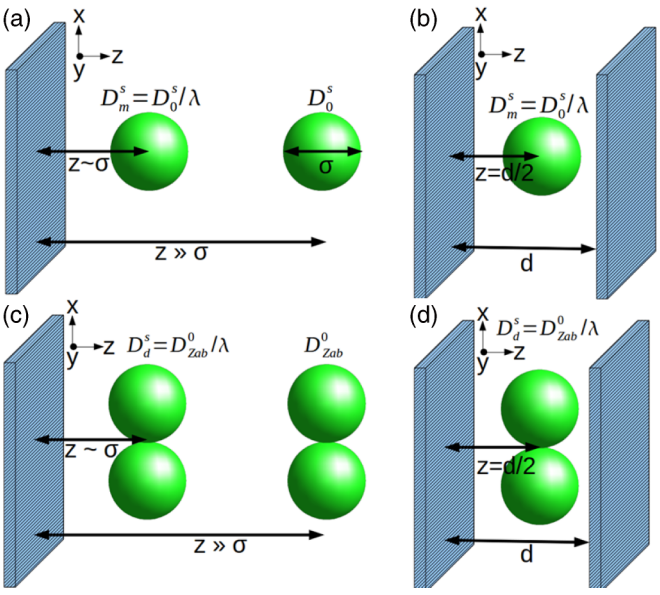

FIG. 2. Cartoon of (a) a sphere of diameter σ far away from and near a flat wall, (b) a sphere confined between two glass plates, (c) a dimer far away from and near a hard wall, and (d) a dimer confined between two plates; the plates are separated by distance d. When the particles are very close to a wall, the short-time diffusion coefficient is hindered and becomes a function of the distance, z, between the center of the particle and the wall. The reduction in the diffusion can be described by the factor $\lambda(z)$ given by Eq. (2).

As mentioned previously, the dynamics of nonspherical colloids is nowadays a challenging topic of paramount importance within the context of condensed matter physics. From the theoretical point of view, recent advances have been achieved by solving the Navier-Stokes equations in the limit of a low Reynolds number, $\mathrm{Re} \ll 1$, for anisotropic particles [27,31]. In particular, Zabarankin [31] calculated the drag force and the resisting torque experienced by a dicolloid-like particle [see Fig. 2(c)] in the bulk (in three dimensions); a dicolloid is a particle formed by the fusion of two spheres. Then, using Zabarankin's approximation together with an approach similar to the one proposed by Rice [28], one can thus estimate the reduction in the short-time diffusion coefficient of the center of mass of a dimer [see Fig. 2(d)]. A reduction of 45% in the short-time diffusion coefficient of the center of mass of a dimer is estimated. One can compare this result with our experimental measurements, also in the limit of low concentrations [low finite concentration; Fig. 1(b)]. The reduction turns out to be only 30% of the bulk value; $D_d^s/\sigma^2 = (0.01587 \pm 5 \times 10^{-5})\ \mathrm{s}^{-1}$. The difference between theory and experiments is larger than in the case of the monomers. This might be linked to two sources that are not taken into account in the theoretical description: (i) the dimer is not located at the center of the glass plates, as we have assumed, and (ii) it is able to rotate out the parallel plane to the walls. Nonetheless, Happel and Brenner [30] also studied the dynamical behavior of a single spheroid located in the middle of two parallel walls. Then, by mapping the characteristic dimensions of the dimer used in the experiments directly to the spheroid, it is possible to find a decrease in the transverse diffusivity of 33% (theory) and 39% (experiments), which is in better agreement with our estimations and measurements.

At low particle concentrations, one can naively assume that the colloid-colloid hydrodynamic forces are negligible. In that limit, Eq. (1) reduces to $D_i^s \approx D_i^0 D_i^w(l)$. Using this expression together with both the calculations and the experimental measurements at low concentrations, we can show that the ratio D_d^s/D_m^s is equal to 0.51. As we see further below, this value is very close to the reference value used to interpret the measurements and simulations at finite concentrations.

IV. COMPUTER SIMULATIONS AND TEMPORAL RESCALING OF THE SHORT-TIME DYNAMICS

To confirm our experimental results at higher concentrations, we have carried out MD simulations of the whole colloidal dispersion taking into account explicitly the solvent molecules; this avoids the use of an approximation for the colloid-colloid hydrodynamic interactions. The simulation results have been produced with the open source MD package

TABLE I. Experimental state points indicated by diamonds in Fig. 1(b).

Sample	Surface fraction ϕ_{area}	Molar fraction x_d	Number of colloids N
a	0.023	0.871	43
b	0.033	0.034	61
c	0.081	0.450	147
d	0.142	0.734	258
e	0.239	0.077	415
f	0.573	0.020	933

ESPResSo [32,33]. In the simulations, we have considered a two-dimensional system made up of monomers and dimers in a bath of smaller particles representing the solvent molecules. All particles interact through a pseudo-hard-sphere model recently proposed by Jover *et al.* [34]; solvent particles have a diameter 10 times smaller than the colloid size and occupy a surface fraction that allows us to match the experimental conditions, however, in a few cases, we have checked that the same results are obtained when the solvent molecules are 20 times smaller (data not shown). Dimers are formed using the rigid bond feature of ESPResSo. At the beginning of the simulation, all particles are randomly distributed in the simulation box and during the runs the center of mass of each particle is constrained to move on the xy plane; i.e., motion along the z direction is not allowed. Simulations are performed in the NVT ensemble using the Langevin thermostat implemented in ESPResSo. The total number of monomers and dimers used in the simulation matches the number of colloids observed in the view field of the experiment (see Table I). Since computer simulation with the explicit inclusion of solvent molecules is a time-consuming task [35], we basically simulate those state points indicated by diamonds in Fig. 1(b) and a few additional points (Table II) in order to, on one hand, study an extended window of concentrations and, on the other hand, to highlight the dependence of the results on the particle composition.

We should point out that the dynamics provided by the MD simulation does not lie in the same temporal regime of the experiments. Nevertheless, it is possible to rescale the MD time to directly compare with the experiments [36,37]. The rescaling consists in replacing the MD time as $t \rightarrow \sqrt{k_B T/M}\,\frac{\sigma}{D_s^0}t$, where M is the mass of a monomer. Hence, we present all the simulation results with this temporal rescaling.

TABLE II. Additional state points studied by means of MD simulations [see Fig. 1(b)].

Surface fraction ϕ_{area}	Molar fraction x_d	Number of colloids N
0.3	0.2	400
0.4	0.3	600
0.45	0.5	400
0.5	0.5	400
0.55	0.5	500
0.6	0.6	900
0.65	0.5	500
0.7	0.2	900

V. DIFFUSION AT FINITE CONCENTRATIONS: COLLOID-COLLOID HYDRODYNAMIC FORCES

The mean-square displacements, $W(t) \equiv \langle(\vec{r}(t) - \vec{r}(0))^2\rangle$, for the monomer and the center of mass of the dimer for the experimental state points indicated in Fig. 1(b) are displayed in Figs. 3 and 4, respectively. As shown in those figures, the MD results clearly display the ballistic [$W(t) \propto t^2$] and diffusive [$W(t) \propto t$] regimes characteristic of the underlying Newtonian dynamics. Overall, one can observe a very good agreement between MD simulations and experiments (see insets in both figures). This confirms that the simulation model captures the colloid-colloid hydrodynamic effects correctly and that the temporal re-scaling of the MD simulations is appropriated. Besides, we should point out that this level of agreement makes evident that the hydrodynamic interactions are indispensable to explain the observed diffusive behavior; otherwise the colloidal dynamics is not captured correctly (data not shown). Furthermore, as expected, one can observe that the monomers diffuse more rapidly than the dimers. Figure 5 shows that the short-time diffusion coefficients of both species decrease monotonically with the concentration following the same trend. This suggests that the effects of the HIs on the short-time diffusion coefficient can be decomposed into two contributions: one that does not depend on the volume fraction, but only on the confinement (as explained above), and a contribution that is a function of the concentration. Figure 5 also indicates that the concentration dependence of the short-time diffusion coefficients has a similar functional form in both species.

As mentioned above, the MSD of the dimers can also be decomposed into two contributions: parallel and perpendicular to the main axis of symmetry. In Figs. 6 and 7 these

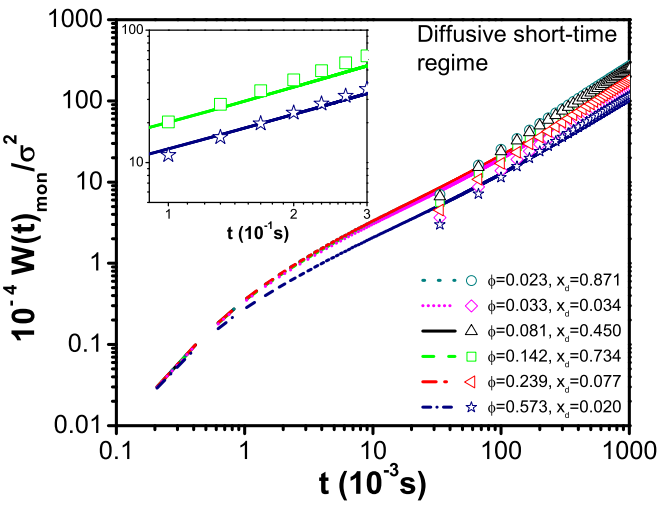

FIG. 3. Mean-square displacement, $W(t)$, of a monomer. Symbols are experimental data and lines simulation results for the state points indicated by diamonds in Fig. 1(b). Inset: Comparison in the short-time regime of two particular cases ($\phi = 0.142$, $x_d = 0.450$ and $\phi = 0.573$, $x_d = 0.020$).

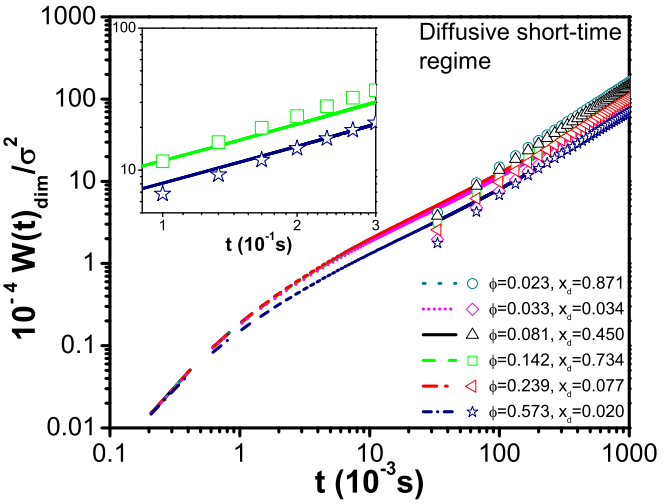

FIG. 4. Mean-square displacement, $W(t)$, of the center of mass of the dimer. Symbols are experimental data and lines simulation results for the state points indicated by diamonds in Fig. 1(b). Inset: Comparison in the short-time regime of two particular cases ($\phi = 0.142$, $x_d = 0.450$ and $\phi = 0.573$, $x_d = 0.020$).

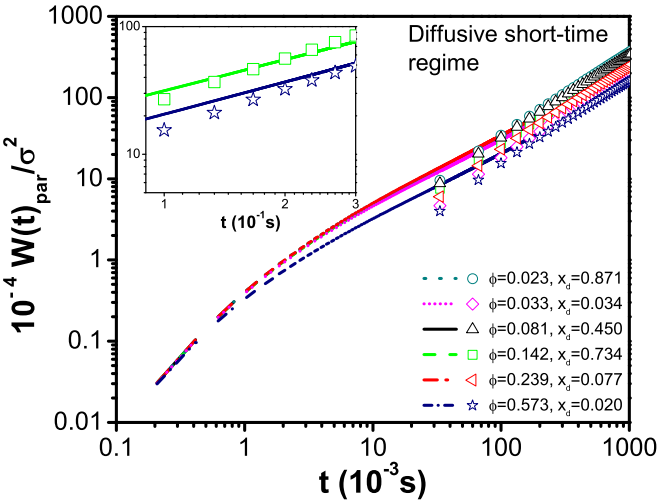

FIG. 6. Mean-square displacement, $W(t)$, for the parallel displacement, with respect to the main axis, of a dimer. Symbols are experimental data and lines simulation results for the state points indicated by diamonds in Fig. 1(b). Inset: Comparison in the short-time regime of two particular cases ($\phi = 0.142$, $x_d = 0.450$ and $\phi = 0.573$, $x_d = 0.020$).

contributions are explicitly displayed for the experimental state points indicated in Fig. 1(b). There, one can appreciate that the short-time diffusion coefficients, parallel and perpendicular, decrease when the concentration increases. One can also note that diffusion along the parallel direction becomes more rapid than that along the perpendicular one. This can be easily understood if one considers that the cross section perpendicular to the axis of symmetry of the dimer is smaller than the parallel one. This means that less solvent molecules collide frontally with the dimer, thus reducing drastically the friction in the parallel direction. The opposite scenario occurs in the perpendicular direction. Nonetheless, at sufficiently long times, i.e., when the dimer has explored most of its phase space, both MSDs reach the same value (data not shown); this behavior will be reported elsewhere [38]. Again, within the time window shown here, the computer simulations are able to capture the whole diffusive mechanisms.

To fully characterize the dynamics of the dimers, we have also measured the mean-square angular displacement, which is explicitly shown in Fig. 8. In this figure, one can observe that the computer simulations predict a mean-square angular displacement that displays a linear time dependence [$W(t)_{\rm rot} \propto t$] at short times of the diffusive regime. In this case, the deviations between simulations and experiments are more notable (see upper-left inset); this difference might be related

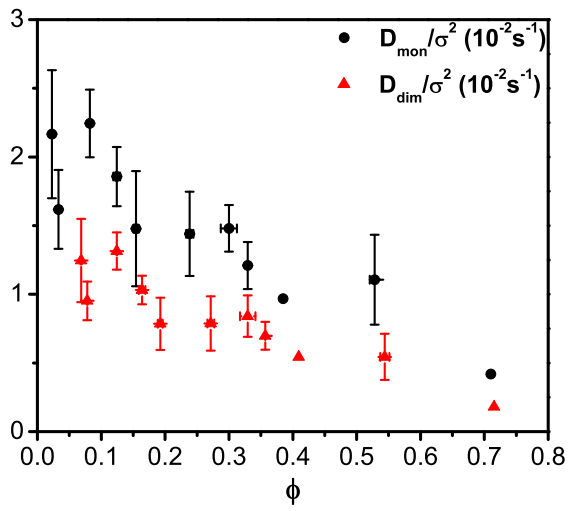

FIG. 5. Experimental short-time diffusion coefficients, D^s, of the sphere and center of mass of the dimer as a function of the total packing fraction obtained from the expression $W(t) = 4D^s t$.

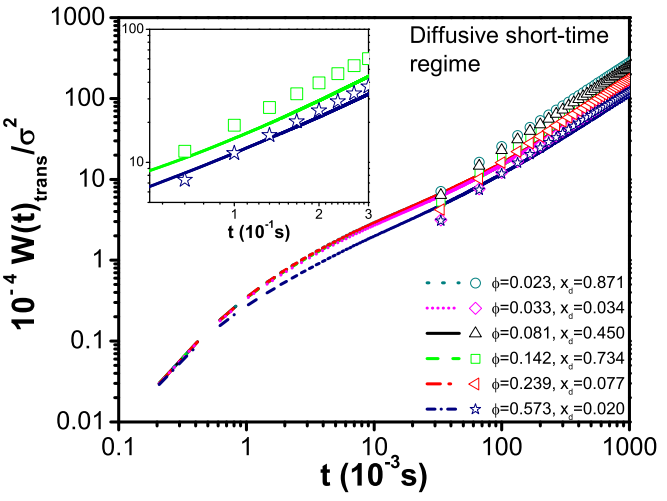

FIG. 7. Mean-square displacement, $W(t)$, for the perpendicular displacement, with respect to the main axis, of a dimer. Symbols are experimental data and lines simulation results for the state points indicated by diamonds in Fig. 1(b). Inset: Comparison in the short-time regime of two particular cases ($\phi = 0.142$, $x_d = 0.450$ and $\phi = 0.573$, $x_d = 0.020$).

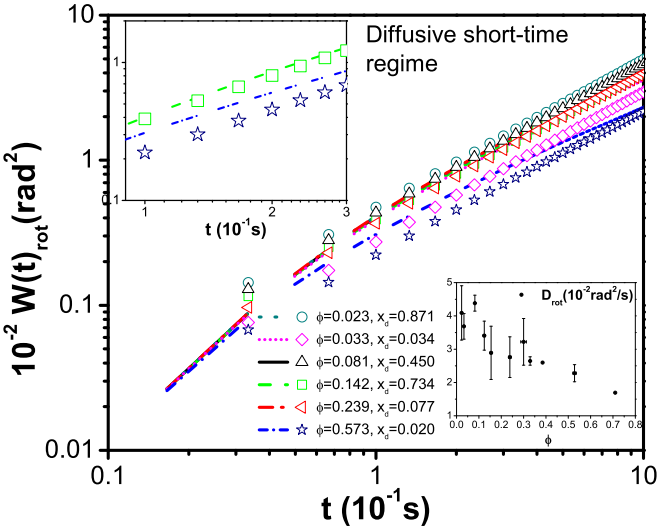

FIG. 8. Mean-square angular displacement of a dimer, $W(t)_{\rm rot}$. Symbols are experimental data and lines simulation results for the state points indicated by diamonds in Fig. 1(b). Top-left inset: Comparison in the short-time regime of two particular cases ($\phi = 0.142$, $x_d = 0.450$ and $\phi = 0.573$, $x_d = 0.020$). Lower-right inset: Experimental concentration dependence of the short-time angular diffusion coefficient.

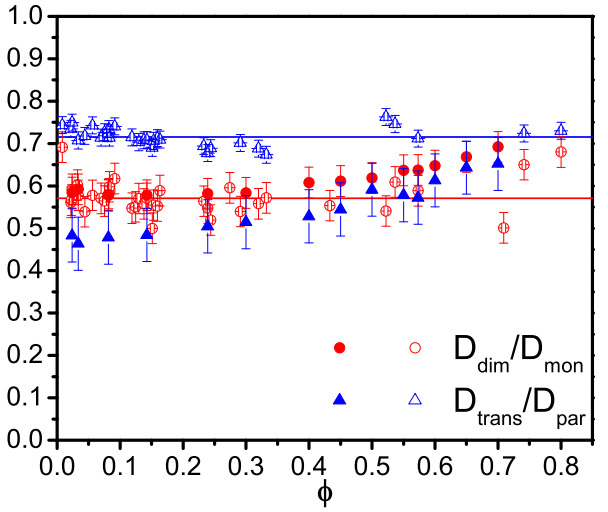

FIG. 9. Experimental (open symbols) and simulation (filled symbols) results for the ratio of the short-time diffusion coefficients of the center of mass of the dimer (dim) and monomer (mon) and the ratio of the transversal (trans) to the parallel (par) short-time diffusion coefficients of the dimer as a function of the total packing fraction. Solid lines are guides for the eye.

to the fact that the temporal rescaling used to compare the simulation data with the experimental results is not completely correct to account for the (slower) rotational dynamics.

VI. DISCUSSION: DECOMPOSITION AND FACTORIZATION

So far, we have characterized the dynamics of both species, i.e., monomers and dimers, over a wide interval of concentrations [see Fig. 1(b)]. As explained above, wall-particle hydrodynamic forces are responsible for the increase in drag force parallel to the walls. This mechanism clearly affects particle diffusion in the parallel plane, but it is an effect that enters each particle in the same way regardless of the species, whereas diffusion in the perpendicular direction is suppressed due to the high degree of confinement of the particles. Thus, the phenomenology observed in the MSDs should be associated with colloid-colloid hydrodynamic forces. As mentioned above, one might think that the latter do not contribute dramatically at low and high particle concentrations but should be important at intermediate concentrations. Additionally, due to the torques that the dimers experience, one might also think that translational-rotational hydrodynamic coupling may drastically affect their dynamical behavior [39]. Therefore, in order to quantify the difference in the diffusivities of monomers and dimers, we consider the ratio of the short-time diffusion coefficients of the centers of mass of the dimer and the monomer. This ratio is explicitly shown in Fig. 9 as a function of the total packing fraction. Interestingly, this ratio is practically independent of both the total packing fraction and the molar fraction of dimers up to packing fractions $\phi \sim 0.5$ and takes the value 0.57 ± 0.03. The latter is close to the value we have determined from Eq. (1) assuming that colloid-colloid hydrodynamic forces are negligible, $D^{\rm cc} \sim 1$, at low concentrations, $D^s/D^0 \sim 0.51$; the computer simulations predict the same dynamical behavior. On the other hand, at higher concentrations, this ratio displays a small but systematic increase. In the experiments, the window of concentrations where this increase is seen is dominated by the contribution of the monomers [see Fig. 1(b)], i.e., $x_d \sim 0.1$. However, the computer simulations performed at dimer molar fraction $x_d = 0.5$ also shows this increase. Thus, the physical scenario observed at high concentrations $\phi > 0.5$ seems to be independent of the particle composition and indicates that HIs might promote either a small increase in the short-time dynamics of the dimers or a small decrease in the short-time dynamics of the monomers.

Overall, our findings suggest that HIs play the following crucial role in the colloidal dynamics of the mixture: their effects on the diffusion coefficients are identical in both species and can be decomposed into a short-time coefficient, including only a confinement contribution, and a monotonically decreasing concentration-dependent part, as proposed originally in Eq. (1).

A similar behavior is also seen for the ratio of the transversal and parallel short-time diffusion coefficients of the dimer, with an experimental value of 0.71 ± 0.02, although in this case the simulations (0.52 ± 0.05) underestimate the value measured in the experiments. This difference might be related to the number of approximations included in the simulation model, which does not take into account several features of the physical system, for example, dimers can slightly rotate along the perpendicular plane of confinement, producing an interaction with the walls.

VII. CONCLUDING REMARKS

We have shown that the ratio of the short-time self-diffusion coefficients in a quasi-two-dimensional colloidal mixture made up of monomers and dimers can be decomposed into two

parts: one that depends only on the degree of confinement and the other that is a function of the colloid-colloid hydrodynamic forces. We particularly have demonstrated that the second contribution is independent of both the composition and the particle concentration up to a packing fraction of 0.50. Our results imply that in this regime of concentrations, the hydrodynamic interactions are equal for both species and factorable. Thus, by characterizing the short-time self-diffusion of one of the species, the other can be straightforwardly determined. However, at higher concentrations, this ratio displayed a small, but systematic increase, pointing to the fact that HIs promote either faster diffusion of the dimers or slower diffusion of the monomers. The computer simulations indicated that such scenario is independent on the particle composition. Nevertheless, further experiments and computer simulations are needed to corroborate the universality of our results in the case of mixtures with either higher size ratios or different shapes. Our findings are thus crucial for the understanding of colloidal dynamics and will serve as benchmark for the development of theoretical frameworks that take into account HIs in anisotropic mixtures at finite concentration.

ACKNOWLEDGMENTS

The authors acknowledge partial financial support from Conacyt (Grants No. 237425 and No. 182132). R.C.-P. also acknowledges the financial support provided by the Marcos Moshinsky fellowship 2013–2014.

[1] J. K. G. Dhont, *An Introduction to Dynamics of Colloids* (Elsevier, Amsterdam, 1996).
[2] G. Nägele, Phys. Rep. **272**, 215 (1996).
[3] J. Kotar, M. Leoni, B. Bassetti, M. C. Lagomarsino, and P. Cicuta, Proc. Natl. Acad. Sci. USA **107**, 7669 (2010).
[4] R. Golestanian, J. M. Yeomans, and N. Uchida, Soft Matter **7**, 3074 (2011).
[5] L. Damet, G. M. Cicuta, J. Kotar, M. C. Lagomarsino, and P. Cicuta, Soft Matter **8**, 8672 (2012).
[6] A. Vilfan and H. Stark, Phys. Rev. Lett. **103**, 199801 (2009).
[7] W. Yang, V. R. Misko, K. Nelissen, M. Kong, and F. M. Peeters, Soft Matter **8**, 5175 (2012).
[8] J. C. Meiners and S. R. Quake, Phys. Rev. Lett. **82**, 2211 (1999).
[9] S. Herrera-Velarde, E. C. Euán-Díaz, F. Córdoba-Valdés, and R. Castañeda-Priego, J. Phys.: Condens. Matter **25**, 325102 (2013).
[10] B. Lin, J. Yu, and S. A. Rice, Phys. Rev. E **62**, 3909 (2000).
[11] S. Bhattacharya, J. Blawzdziewicz, and E. Wajnryb, J. Fluid Mech. **541**, 263 (2005).
[12] M. D. Carbajal-Tinoco, Lopez-Fernandez, and J. L. Arauz-Lara, Phys. Rev. Lett. **99**, 138303 (2007).
[13] X. Xu, S. A. Rice, B. Lin, and H. Diamant, Phys. Rev. Lett. **95**, 158301 (2005).
[14] K. Zahn, J. M. Méndez-Alcaraz, and G. Maret, Phys. Rev. Lett. **79**, 175 (1997).
[15] J. Santana-Solano and J. L. Arauz-Lara, Phys. Rev. Lett. **87**, 038302 (2001).
[16] J. Santana-Solano, A. Ramírez-Saito, and J. L. Arauz-Lara, Phys. Rev. Lett. **95**, 198301 (2005).
[17] A. L. Thorneywork, R. E. Rozas, R. P. A. Dullens, and J. Horbach, Phys. Rev. Lett. **115**, 268301 (2015).
[18] Y. Han, A. M. Alsayed, M. Nobili, J. Zhang, T. C. Lubensky, and A. G. Yodh, Science **314**, 626 (2006).
[19] K. V. Edmond, M. T. Elsesser, G. L. Hunter, D. J. Pine, and E. R. Weeks, Proc. Natl. Acad. Sci. USA **109**, 17892 (2012).
[20] A. Wang, T. G. Dimiduk, J. Fung, S. Razavi, I. Kretzschmar, and V. N. Manoharan, J. Quant. Spectrosc. Radiat. Transfer **146**, 499 (2014).
[21] D. T. Valley, S. Rice, B. Cui, H. Diamant, and B. Lin, J. Chem. Phys. **126**, 134908 (2007).
[22] D. J. Kraft, R. Wittkowski, B. ten Hagen, K. V. Edmond, D. J. Pine, and H. Löwen, Phys. Rev. E **88**, 050301(R) (2013).
[23] M. M. Panczyk, N. J. Wagner, and E. M. Furst, Phys. Rev. E **89**, 062311 (2014).
[24] M. Medina-Noyola, Phys. Rev. Lett. **60**, 2705 (1988).
[25] A. Garcia-Castillo and J. L. Arauz-Lara, Phys. Rev. E **78**, 020401(R) (2008).
[26] J. C. Crocker and D. G. Grier, J. Coll. Interf. Sci. **179**, 298 (1996).
[27] M. De Corato, F. Greco, G. D'Avino, and P. L. Maffettone, J. Chem. Phys. **142**, 194901 (2015).
[28] B. Lin, J. Yu, and S. A. Rice, Coll. Surf. A **174**, 121 (2000).
[29] H. Brenner, Chem. Eng. Sci. **16**, 242 (1961).
[30] J. Happel and H. Brenner, *Low Reynolds Number Hydrodynamics* (Kluwer, Dordrecht, 1983).
[31] M. Zabarankin, Proc. R. Soc. A **463**, 2329 (2007).
[32] H. J. Limbach, A. Arnold, B. A. Mann, and C. Holm, Comput. Phys. Commun. **174**, 704 (2006).
[33] A. Arnold, O. Lenz, S. Kesselheim, R. Weeber, F. Fahrenberger, D. Röhm, P. Košovan, and C. Holm, ESPResSo 3.1—Molecular dynamics software for coarse-grained models, in *Meshfree Methods for Partial Differential Equations VI*, Lecture Notes in Computational Science and Engineering, Vol. 89, edited by M. Griebel and M. A. Schweitzer (Springer, Berlin, 2013), pp. 1–23.
[34] J. Jover, A. J. Haslam, A. Galindo, G. Jackson, and E. A. Müller, J. Chem. Phys. **137**, 144505 (2012).
[35] A. Torres-Carbajal, S. Herrera-Velarde, and R. Castañeda-Priego, Phys. Chem. Chem. Phys. **17**, 19557 (2015)
[36] L. López-Flores, H. Ruíz-Estrada, M. Chávez-Páez, and M. Medina-Noyola, Phys. Rev. E **88**, 042301 (2013).
[37] G. Pérez-Angel, Sánchez-Díaz, P. E. Ramírez-González, R. Juárez-Maldonado, A. Vizcarra-Rendón, and M. Medina-Noyola, Phys. Rev. E **83**, 060501(R) (2011).
[38] J. R. Villanueva-Valencia *et al.* (unpublished).
[39] A. Neild, J. T. Padding, L. Yu, B. Bhaduri, W. J. Briels, and T. W. Ng, Phys. Rev. E **82**, 041126 (2010).